Joint Session (Hydrography and Baltic Fish Committee)
Interaction between Physics and Fish in the BAltic (C+J)
C M 1996/C+J:1

The mesoscale variability of nutrients and plankton as seen in a coupled model

Wolfgang Fennel and Thomas Neumann
Institut für Ostseeforschung Warnemünde
an der Universität Rostock
D-18119 Warnemünde, Germany

Abstract

The effect of the variability of mesoscale current patterns on the dynamics of nutrients and plankton is studied by means of a simple coupled model. A chemical-biological model in conjuction with a high resolution circulation model is applied to the southwestern Baltic. The biological model has four state variables, a limiting nutrient, phytoplankton, zooplankton and detritus. The circulation model is based on an implementation of the GFDL-model in the modular version (MOM 1).
Experimental simulations of a spring bloom with the coupled model show the generation of patchiness, which is basically controlled by the mesoscale circulation patterns in conjunction with sinking of plankton and nutrient limitation. The exchange of material among the sub-basins of the model area is briefly discussed.

1 Introduction

The dominant signal in the circulation of the Baltic Sea is the mesoscale variability which is basically forced by winds and pressure gradients. River discharges play only a minor role as driving forces but are important for maintaining the mean salinity gradients and as sources of nutrients. The characteristic time scales of the mesoscale processes are 2 to 5 days, i.e., the time scale of weather patterns. The spatial scales are the internal Rossby radii, which vary seasonally and regionally, Fennel, Seifert and Kayser (1991), and the horizontal scales of topographic features such as sills and trenches.
The mesoscale processes affect the dynamics of nutrients and plankton in many ways: Mesoscale current patterns redistribute matter within the basins and control the distribution of riverine material in the coastal zone and its transports into the basins. Coastal upwelling and topographically induced upward flows affect the vertical fluxes of nutrients.
The Baltic is known as one of the most intensively observed marine areas. There are large data sets comprising physical, chemical, geological, and biological data. However, caution has to be exercised when using such data owing to the problem of observational undersampling. Many data are gathered during monitoring cruises where a number of stations were visited at a regular time scheme but often without consideration of the mesoscale variability. Improved observational strategies requires the linkage of measurements and theory. A prerequisite for this linkage is the availability of numerical models.
A horizontally integrated physical-biogeochemical model of high vertical resolution for the Baltic Sea proper was developed by Stigebrandt and Wulff (1987) to compute the dynamics of the mixed layer and the patterns of primary production, nutrients, and oxygen for a 20 year period. A review of the state of the art of the ecological modelling of the North Sea and the Baltic Sea was given by Fransz, Mommaerts, and Radach (1991).
The next step consists in the connection of high resolution circulation models and biological-chemical

models. The feasibility to integrate biological models into general circulation models was shown for example by Sarmiento, Slater, Fasham, Ducklow, Toggweiler, and Evans (1993) and Slater, Sarmiento, and Fasham (1993). These studies are based on the GFDL general circulation model and the biological model developed by Fasham, Ducklow, and McKelvie (1990) and were focussed on the nitrogen cycling in the North Atlantic euphotic zone. Physical chemical biological models of the North Sea were presented recently by Aksnes et al. (1995) in order to simulate the plankton development form February to June 1988, and by Moll (1995) in order to describe the yearly cycle of the primary production in different parts of the North Sea. However, the spatial resolution of these models is rather coarse, ($20\,km$).
In this paper we combine as a first step towards a three dimensional ecosystem model of the Baltic a simple chemical-biological model and a highly resolved circulation model, which is able to describe mesoscale patterns. The high resolution regional model of the southwestern Baltic based on the modular version of the Bryan-Cox primitive equation circulation model, MOM 1, described in Pacanowski, Dixon and Rosati (1990). The biological dynamics is based on the model of Fennel (1995) which is relative simple but describes the yearly cycle of nutrients and plankton in a reasonable way.
The present study is focussed on the simulation of a spring bloom in the south western Baltic to understand how circulation and biological dynamics interact to generate distribution patterns of plankton and how these patterns vary with time. Experimental simulations allow to estimate how the locations of monitoring stations have to be chosen in order to reduce the problems of observational undersampling.

2 A coupled model

In the following we use the Modular Ocean Model (MOM 1) which is a rewritten version of the primitive equation ocean model of Bryan and Cox (GFDL-model). The model is adapted to the southwestern Baltic Sea with a horizontal grid scale of $1.856\,km$, (1 nautical mile), and a vertical resolution of $2\,m$ for the first 12 layers and then a gradually increasing thickness of the layers for increasing depth. Owing to the high resolution this eddy resolving, baroclinic model is able to produce mesoscale current patterns which evolve in response to the wind, see e.g. Fennel and Seifert (1995).
The MOM 1 has built in options for additional tracers which allow to incorporate the biological dynamics in a straightforward manner. The biological dynamics is introduced by means of the model of Fennel (1995), which was designed to model the behaviour of nutrients and plankton with a minimum number of state variables and which applies for sub-basins of the Baltic Sea.
In order to save computer time we use the rigid lid approximation which filters out the surface gravity waves, and we close the model area by straight walls. The artificial walls affect the mesoscale variability mainly close to the walls with a scale set by the first mode baroclinic Rossby radius.
The horizontal turbulent viscosities and diffusivities, which are relevant for momentum and tracers, respectively, are assumed to be constant. For the vertical mixing we use the Richardson-number model of Pacanowski and Philander (1981), which is implemented in the MOM 1. The model area and the bathymetry is shown in fig. 1. The initial distribution of salinity and temperature was derived from the data set of the monitoring cruise of the Institut für Ostseeforschung (IOW) in March 1992.
We consider only a limited period of about 80 days to cover the spring bloom. The model is forced by wind and solar radiation. We start with a prescribed pre-spring stratification and force the development of a thermocline through the solar radiation, I_0, which reaches the sea surface, see e.g. Brock (1981).
For the corrections due to cloudiness and albedo we adopt the empirical formula of Smith and Dobson (1984). For the details we refer to the paper of Smith and Dobson (1984). For the albedo we use a constant value, 0.1, and the cloudiness is related to the wind direction in a simple manner, (full cloud cover for northerly and southerly winds, medium cover for westerly winds and no clouds for easterly winds). For the biological dynamics four state variables are taken into account: limiting nutrient, (N), phytoplankton, (P), zooplankton, (Z), and detritus, (D).
The biological state variables are given as concentrations relative to a reference concentration of the limting nutrient, N_{ref}, which is set by the winter value of nitrogen. The equations for the biological state variables are explicitly

$$\begin{aligned}\frac{\partial}{\partial t}N + \mathbf{v}\cdot\nabla N - A\Delta N &= -\frac{r N^2 P}{\alpha^2 + N^2} + L_{PN}(P - P_0) \\ &\quad + L_{ZN}(Z - Z_0) + L_{DN}D, \qquad (1)\end{aligned}$$

$$\frac{\partial}{\partial t}P + \mathbf{v}\cdot\nabla P + w_{SP}\frac{\partial}{\partial z}P - A\Delta P = \frac{r N^2 P}{\alpha^2 + N^2} - \beta(1 - exp(-I_v^2 P^2))\, Z - L_P(P - P_0), \quad (2)$$

$$\frac{\partial}{\partial t}Z + \mathbf{v}\cdot\nabla Z - A\Delta Z = \beta(1 - exp(-I_v^2 P^2))\, Z - L_Z(Z - Z_0), \quad (3)$$

$$\frac{\partial}{\partial t}D + \mathbf{v}\cdot\nabla D + w_{SD}\frac{\partial}{\partial z}D - A\Delta D = L_{PD}(P - P_0) + L_{ZD}(Z - Z_0) - L_{DN}D. \quad (4)$$

Here w_{SD} and w_{SP} are the sinking speeds of dead and alive particles, respectively, where we assume that dead particle sink faster $w_{SD} = -4\,m/s$ than the plankton cells $w_{SP} = -1\,m/s$. These sinking speeds are in the range of the more refined approaches used in Stigebrandt and Wulff (1987) and in Aksnes et al. (1995). As shown by Bodungen et al. (1981) the sinking does occur event-like rather as a steady process. Thus the sinking is taken into account in an effective manner only.
The role of light is included in the growth rate, r. The solar radiation at the sea surface is given by the same formula used for the heating of the upper layer. However, only half of the incoming radiation can be used for photosynthesis, $PAR = I_0/2$, where PAR is the photosynthetically active radiation. The rate r is given by

$$r = r_{max}\, PI(t, \mathbf{r}). \quad (5)$$

We use the PI formula of Steele (1962),

$$PI(t, x, y, z) = \frac{I(t, x, y, z)}{Iopt}\exp\Big(1 - \frac{I(t, x, y, z)}{Iopt}\Big) \quad (6)$$

Here $I(t, \mathbf{r})$ is controlled by the light attenuation due to the water and the light attenuation due to self-shading of phytoplankton.

$$I(t, x, y, z) = PAR\exp\Big(k_w\, z - k_c \int_z^0 P(t, x, y, z')dz'\Big), \quad (7)$$

where the attenuation constant of the water is chosen $k_w = 0.15\,1/m$ and for the self-shading effect, $k_c = 0.03\,1/m$. For I_{opt} we adopt the value given by Stigebrandt and Wulff (1987),

$$I_{opt} = max(\frac{I_0}{4}, I_{min}), \quad (8)$$

where $I_{min} = 25\,W/m^2$.
The loss rates L_{PN}, L_{ZN},L_{PD}, and L_{ZD} specify how much of the losses of phytoplankton, L_P, and zooplankton, L_Z, is transferred to nutrients, N, and detritus, D, i.e.,

$$L_P = L_{PN} + L_{PD},$$
$$L_Z = L_{ZN} + L_{ZD}.$$

The rate L_{DN} prescribes the recycling of detritus to nutrients. The grazing is modelled by a modified Ivlev formula $\beta(1 - exp(-I_v^2 P^2)$ where β is the maximum grazing rate and I_v a so-called Ivlev constant. The background values P_0 and Z_0 are the winter concentrations, which serve as initial values at the onset of the vernal bloom. The mortality which is included in the rate L_{PD} (transfer of plankton to detritus) is assumed to be larger below the photic zone than within the upper part of the water column.
Before the onset of the spring bloom the nutrients are set to the winter value, i.e., the maximum. We assume also a high start value of the detritus. During the initialization the detritus sinks down and forms a bottom pool which is slowly converted into nutrients. The numerical values of the relevant parameters and the initially values of the state variables are listed in table 1.
In order to convert the relative values of the state variables to the more familar absolute values we multiply the model nutrient concentration by N_{ref}, i.e., $N^{absolute} = N^{model} N_{ref}$. The model phytoplankton can be expressed in units of chlorophyll-a by using the Redfield ratio to express P in carbon units and then using a carbon to chlorophyll-a ratio of 50/1.

Table 1: model parameters

parameter	meaning	numerical value
N_{ref}	reference value of limiting nutrient	$4.5 mmol N/m^3$
N_0	initial value of N	1
P_0	background of P	0.005
Z_0	background of Z	0.005
D_0	initial value of D	1
w_{SD}	sinking of D	$-5\,m/d$
w_{SP}	sinking of P	$-1\,m/d$
L_{DN}	recycling of D to N	$0.003/d$
L_{PD}	transfer of P to D in photic zone below photic zone	 $0.02/d$ $0.1/d$
L_{PN}	transfer of P to N	$0.01/d$
L_{ZD}	transfer of Z to D	$0.02/d$
L_{ZN}	transfer of Z to N	$0.01/d$
I_v	Ivlev constant	1.1
β	maximum grazing	$0.5/d$
r_{max}	maximum uptake rate	$1/d$
α	half-saturation	0.3
A_H	horizontal eddy viscosity	$10^5 cm^2/s$
A_{TH}	horizontal eddy diffusivity	$10^5 cm^2/s$

3 Simulation of plankton and nutrients distributions

The model is used to simulate the spatial distribution of the state variables during a spring bloom. The distribution patterns of the chemical and biological state variables are known to have patchy structures, see e.g. Dybern and Hansen (1989).

In order to initialize the model we run the model for 5 days forced by a constant westly wind and using an initial distribution of temperature and salinity fields derived from data of March 1992. Then we start the heating by solar radiation, corresponding to the first day of March, and applied a varying wind as shown in fig. 2. During the initialization the the state variables P and Z are set to the background values and N assumes its winter value as listed in table 1. The initial value of D was set to the same value as N. During the initialization the detritus sinks to the bottom and forms a pool of material which is slowly converted into nutrients.

Physical processes

The formation of the thermocline is shown in fig. 3 where by means of a time series of vertical temperature profiles at the station AS1 in the central Arkona Sea, see fig. 1. The thermocline development commenced during day 20 to 30. The depth of the mixed layer is controlled by the magnitude of the wind.

In response to the wind a rich spectrum of mesoscale current patterns is generated. Coastal jets associated with up- and downwelling are driven by longshore winds. Due to the existence of coastal boundaries a recirculation of the Ekman transport establishes below the upper mixed layer and interacts with the bottom topography. Mesoscale features like eddies and filaments are shed by the coastal flows or are generated at topographical features.

In order to illustrate the mesoscale patterns we discuss briefly the example of the flow regimes at day 63, which was generated by the onset of easterly winds at day 60. The surface current is shown in fig. 4(a). At the southeast coast a coastal jet has developed which do not enter the Pomeranian Bight but is deflected off-shore towards northwest and follows roughly the $20\,m$ isobath. In the Pomeranian Bight we recognize

an off-shore surface current in the eastern part and a slight coastal current in the western part.
A strong coastal jet exists also at the northern boundary off the swedish coast. A big anticyclonic eddy has developed in the central Arkona Sea. A further pair of eddies can be seen at the southern end of the Rønne bank.
In fig. 4(b) the currents in $9\,m$ depth are shown. The coastal jets and the eddies described above have a similar structure as near the surface. However, the current in the eastern part of the Pomeranian Bight flows alongshore and is connected with the coastal jet. The $19\,m$ level is shown in fig. 4(c). The anticyclonic eddy in the Arkona Sea is and the topographical steering of the flows at the Rønne bank is clearly shown.

Model phytoplankton and nutrients

The development of the model phytoplankton at the sea surface is visualized by a series of snapshots of the model phytoplankton concentration in fig. 5. The bloom evolves first in the shallow coastal areas. This is shown in fig. 5(a) where the surface concentration of the model phytoplankton at day 35 is displayed. Since in the initial phase the bloom is controlled by the sinking, the model phytoplankton remains in the photic zone which stretches over the whole water column in the shallow areas.
At day 38 the bloom develops also in off-shore areas, fig. 5(b). Easterly winds forces an off-shore Ekman transport in the Pomeranian Bight which moves the model plankton away from the coast. After 50 days of model time, the bloom of the model phytoplankton has reached the maximum level in the off-shore areas, as shown in fig. 5(c). Peak values are found in the shallow areas of the southern coast. These high concentrations result from the accumulation of matter caused by the current fields and are biologically driven due to the shallowness of that area, which prevents the model phytoplankton to sink out of the photic layer.
After the peak of the bloom the development of the model plankton is controlled by sinking and nutrient limitation. The model phytoplankton concentration at the sea surface decreases rapidly in the off-shore areas, and the distribution becomes more patchy, see fig. 5(d), where the surface concentration is shown for day 60. In particular, mesoscale features like eddies can keep relatively high concentrations where the anticyclonic eddy in the central Arkona basin, compare fig. 4, is visible in the model phytoplankton concentration. In fig. 6 the model nutrient concentration at the sea surface is shown for the day 51 and day 60. The pictures indicate clearly, that the anticylonic eddy is supplied with nutrients from the coastal zone off the southern swedish coast, and, therefore, a relativelly high phytoplankton concentration can be maintained.
During the bloom period the nutrients in the photic layer are consumed by the phytoplankton and, therefore, the nutrient concentration is low where the phytoplankton concentration is high. This inverse behaviour is shown in fig. 7, where time series of the vertical profiles of the model concentration of phytoplankton and nutrients computed at station AS1 in the central Arkona Sea are plotted. In the upper layer the model plankton increases by growth but decreases by sinking. A peak develops in the thermocline. The model nutrient concentration decreases rapidly in the upper layer but only slowly within the thermocline, fig. 7(b). This implies that the physical and the biological dynamics included in the model are sufficient to generate the well known 'deep maximum' in the thermocline. The 'deep maximum' is generated by the sinking of the model phytoplankton and the diffusive leakage of model nutrients into the photic zone from below.
After the peak of the bloom the nutrient limitation becames crucial and the model phytoplankton concentration increases where nutrients are brought up by mesoscale circulation processes, in particular coastal upwelling. A further mechanism of nutrient injections into the upper layer is the erosion of the thermocline in response to enhanced wind strength. The increased wind speed at day 75, see fig. 2, provides an entrainment of nutrients into the upper layer from below which in turn increases the model phytoplankton concentration, as shown in fig. 7.
A zonal section of the vertical distribution of the model phytoplankton at day 59 along $54,8°$N shows the high values in the thermocline, see fig. 8. Moreover, at the topographical features we observe an enhancement of the model phytoplankton, which can be attributed to an upward transport of nutrients through topographically induced upwelling.
The result of the integration of the model phytoplankton and nutrients over the upper $14\,m$ of the whole model area are shown in fig. 9. The response behaviour of the integrated quantities corresponds to the results of the box model, Fennel (1995), which was used to set up the 'biological dynamics'.

Mean values versus local values

The model results can be used to look at the budgets in different sub-basins of the model area. We devide the model area into four sub-basins with different bathymetries as indicated in fig. 1: the Arkona Sea, the Pomeranian Bight, the Bornholm Sea, and the Mecklenburg Bight. The behaviour of the integrated model phytoplankton varies in the different parts of the model areas. This is shown in fig. 10 where the development of the mean values of the model phytoplankton in the sub-basins are shown. In the shallower parts the mean values are significantly higher than in the deeper off-shore areas.

In order to estimate the degree of representativity of a few selected stations for estimates of the total amount of nutrients and phytoplankton in a whole area we compare the model results integrated over the Arkona Sea with the local concentrations at stations stations, AS1, AS2, and AS3 in the central Arkona Sea, as indicated in fig. 1, where the location of the station AS1 corresponds to the monitoring station 113. The result is shown in fig. 11.

It appears that the basin mean values of the model phytoplankton are larger than those at the local stations. However, there are also events where the local values exceed the mean values. These events are related to the input of nutrients into the photic zone by horizontal advection or vertical mixing. An example of advective transport of nutrients originating from coastal upwelling and being catched in the anticyclonic eddy, see fig. 4, which carries high nutrient concentrations. A similar picture follows from the station BS in the Bornholm Sea, fig. 12(a), while for the station PB in the shallow area of the Pomeranian Bight the magnitudes of mean and local values are compareable but the variability of the local values is rather high, fig. 12(b).

Similarily we compare the mean value of the nutrients with the local values at the stations. The results are shown in fig. 13. Contrary to the model phytoplankton concentrations, the local values of the model nutrients concentrations at the stations are higher than the mean value over the sub-basin. This behaviour can be understood by the fact that after the start of the vernal bloom the model plankton concentrations are high but the nutrients low in the shallower areas. Therefore, using only the open sea stations to describe mean values in a sub-basin underestimates the plankton and overestimate the nutrient concentrations.

Exchange among the sub-basins

Next we look at the problem how matter is exchanged among the subbasins. To this end we express the total mass of the nitrogen in the state variables within the water column. Using the winter concentration of anorganic nitrogen (nitrate, nitrite, and ammonium), $N_{ref} = 4.5\, mmol/m^3$, see Nehring and Matthäus (1991), we find for example for the Arkona Sea a total amount of $m_{AS} = 30 \cdot 10^3$ tons before the start of the spring bloom.

In order to show this the differences to the total initial amount of nitrogen in the different subbasins are plotted versus the model time fig. 14. The simulated scenario suggests that the Bornholm Sea gains a substantial amount of matter, which is transported into the relatively deep Bornholm Sea and sinks to the bottom where it accumulates. This implies that the Bornholm Sea is a deposition area. There is a intense exchange between the Arkona sea and the Pomeranian Bight which varies with a time scale of several days, which is the time scale of the wind forcing.

4 Summary and outlook

Experimental simulations with a coupled physical and biological model show that the generation of phytoplankton patchiness during and after the spring bloom. A chemical-biological model in conjunction with a high resolution circulation model was applied to the southwestern Baltic. The spring bloom commenced in the shallow coastal areas where the model phytoplankton does not sink out of the photic zone. In offshore regions the bloom starts after the formation of the thermocline in response to heating through increased solar radiation.

After the peak of the spring bloom the distribution patterns of the model concentrations of phytoplankton and nutrients are controlled by coastal upwelling as well as mesoscale features such as eddies and filaments which generate or disintegrate patches of the model phytoplankton. The levels in the surface layer are low in the off-shore areas but the model produces a well pronounced plankton peak within the thermocline.

Experimental simulations with such a coupled model allow to estimate the representativity of single stations for estimates of the mean concentrations of sub-basins. This reflects situations where attempts

are made to produce overall budgets from data of a few stations, which as a rule are expected to be undersampled. The simulations showed that the vertical mean of the model phytoplankton concentration at arbitrary stations in the Arkona Sea and the Bornholm Sea are smaller than mean value over the sub-basins. However, in the shallow area of the Pomeranian Bight the local values are quite close to the mean value.

The mean values of the model phytoplankton concentration show a different time behaviour in the different sub-basins of the model area. This depends on the different bathymetries of the sub-basins as well as on the exchange of matter among the basins. These differences indicate the problem of deriving rates, needed in the equations of the biological dynamics, from data sets. Obviously, a good approach is to use data sets from the central basins and to concentrate on integrated quantities such as response times and relative order of magnitude rather than fitting the model to a specific data set.

This study is a further step towards a ecosystem model of the Baltic Sea insofar as it provides a coupling of mesoscale dynamics and plankton dynamics. The present investigation is a feasibility study which showed that the redistribution of plankton and nutrients by mesoscale circulation patterns can be described by means of a model with high spatial resolution.

As next steps several subsequent improvements are envisaged. The circulation model can be expanded to the whole Baltic Sea. The chemical-biological model can be refined in several ways: Processes summerized under the different rates can be resolved in more detail. More state variables such as different species and limiting substances can be taking into account. Benthic processes and inputs of nutrients through rivers and the atmosphere can be included. This requires step by step upgrades which can be achieved by interdisciplinary efforts. Results of the coupled modelling can be used also to address new questions to the observations and can help to design observational campaigns to reduce the undersampling problem.

References

Aksnes,D.,L., K.B.Ulvestad, B.M.Balino, J.Berntsen, J.K.Egge, and E.Svendsen (1995): "Ecological modelling in coastal waters: towards predictive physical-chemical-biological simulation models". Ophellia, **41**, 5-36.

Bodungen,B., K.Bröckel, V.Smetacek, and B.Zeitschel (1981): "Growth and sedimentation of the phytoplankton spring bloom in the Bornholm Sea". Lieler Meeresforsch., Sonderh. 5, 49-60.

Brock, T.D. (1981): "Calculating solar radiation for ecological studies". Ecol. Model., **14**, 265-293.

Dybern, B.I. and P.Hansen (Eds.) (1989):"Baltic Sea Patchiness Experiment -PEX 86-". ICES, Cooperative Research Report, No. 163, Copenhagen, (2 volumes)

Fasham, M.J.R, H.W.Ducklow , and D.S.McKelvie (1990):" A nitrogen- based model of plankton dynamics in the oceanic mixed layer". Jour. Mar. Res., **48**, 591-639.

Fennel, W. (1995): "Model of the yearly cycle of nutrients and plankton in the Baltic Sea". Journal of Marine Systems, 6, 313-329.

Fennel,W., T.Seifert, and B.Kayser (1991):"Rossby radii and phase speeds in the Baltic Sea". Continental Shelf Research, **11**, 23-36.

Fennel,W. and T.Seifert, (1995): "Kelvin wave controlled upwelling in the western Baltic". Journal of Marine Systems, 6, 289-300.

Fransz,H.G., J.P.Mommaerts, and G.Radach (1991): "Ecological modelling of the North Sea". Netherland Jour. Sea Res., **28**, 67-140.

Moll,A. (1995): " Regionale Differenzierung der Primärproduktion in der Nordsee: Untersuchungen mit einem drei-dimensionalen Modell". Ber. ZMT, Univ. Hamburg, Nr. 19, pp151.

Nehring,D., and W.Matthäus (1991): "Die hydrographisch-chemischen Bedingungen in der westlichen Ostsee im Jahre 1991". Dt. Hydrogr. Z., **44**, 217-238.

Pacanowski,R.C., and S.G.H. Philander 1981. "Parameterization of the vertical mixing in numerical models of the tropical ocean". J.Phys.Oceanogr., **11**, 1443-1451.

Pacanowski,R.C., K.Dixon and A.Rosati (1990): "The GFDL modular ocean model users guide version 1.0". GFDL Group Technical Report No. 2. Geophysical Fluid Dynamics Laboratory, NOAA, Princeton Univ., Princeton, variously paged.

Sarmiento,J.L., R.D.Slater, M.J.R.Fasham, H.W.Ducklow, J.R.Toggweiler, and
G.T.Evans (1992): "A seasonal three-dimensional ecosystem model of nitrogen cycling in the North Atlantic euphotic zone". Global biogeochemical cycles, **7**, 417-450.
Slater, R.D., J.L.Sarmiento, and M.J.R.Fasham, (1993): "Some parametric and structural simulations with a three-dimensional ecosystem model of nitogen cycling in the North Atlantic euphotic zone". In:"Towards a model of ocean biogeochemical processes". G.T.Evans and M.J.R. Fasham (Eds.), Springer, Berlin, 261-294.
Smith,S.D., and F.W.Dobson (1984): "The heat budget at Ocean Weather Station Bravo". Atmos.-Ocean., **22**, 1-22.
Steele, J. (1962): "Environmental control of photosynthesis in the sea." Limnol. Oceanogr., **7**, 137-150.
Stigebrandt, A. and F. Wulff (1987):" A model for the nutrients and oxygen in the Baltic proper". Journal of Marine Research, **45**, 729-759.

Figure Captions

fig. 1: A map of the southwestern Baltic with AS-Arkona Sea, MB-Mecklenburg Bight, PB-Pomeranian Bight, and BS-Bornholm Sea. In the central Arkona Sea the stations AS1, AS2, and AS3, in the Bornholm Sea the station BS and and the Pomeranian Bight the station PB are indicated for later reference. The station AS1 corresponds to the monitoring station 113. The model area is indicated by the box.

fig. 2: Time series of the synthetical wind used to the circulation model.

fig. 3: Time series of vertical model temperature profiles in the central Arkona Sea, at the station AS1.

fig. 4: Mesoscale circulation pattern at day 63 at the surface (a), in 9 m depth (b), and in 19 m depth (c). The reference arrow (bottom left corner) corresponds to $30\,cm/s$.

fig. 5: A series of snapshots of the surface distribution of model phytoplankton for (a) day 35, (b) day 38, (c) day 50, and (d) day 60.

fig. 6: Nutrient distribution at the sea surface for day 51 (top) and day 60 (bottom).

fig. 7: Time series of vertical profiles of the model nutrients (a) and phytoplankton (b) at the station AS1 in the Arkona Sea. The profiles are taken every 12 hours (midnight and noon) and subsequently shifted by a constant offset.

fig. 8: Zonal-vertical section of the plankton distribution along $54,8°N$ at day 59 showing the deep plankton maximum in the thermocline. Note also the higher levels of P over the topographic features.

fig. 9: The temporal development of the concentrations of the model nutrients, N (solid), and model phytoplankton, P (dashed), integrated over the upper $14\,m$ of the whole model area.

fig. 10: Development of the mean concentration of the model phytoplankton of the different sub-basins, Bornholm Sea (solid), Arkona Sea (dashed), Mecklenburg Bight (dotted), and Pomeranian Bight (dashed-dotted).

fig. 11: Time series of the mean value of the model phytoplankton in the Arkona Sea (dashed) and of the vertical means at the stations AS1, AS2, and AS3.

fig. 12: Time series of the mean value of the model nutrient concentration in the Arkona Sea (dashed) and of the vertical means at the stations AS1, AS2, and AS3.

fig. 13: As fig. 11, but for the stations BS and PB.

fig. 14: Temporal development of the differences of the total masses (in nitrogen) in the different sub-basins relative to the initial mass (BS-solid; AS-dashed, PB-point-dashed, MB-points).

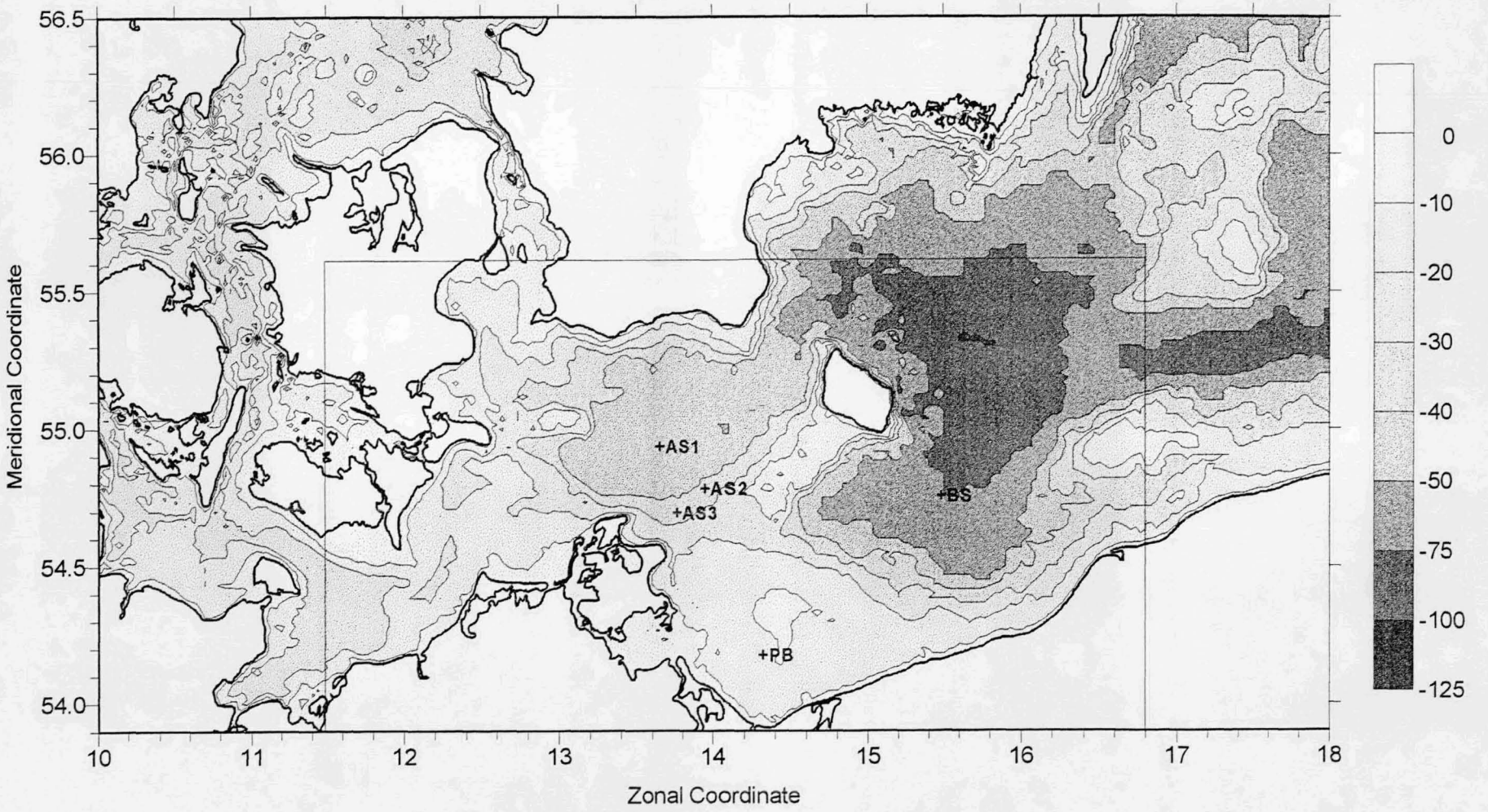

fig. 1: A map of the southwestern Baltic with AS-Arkona Sea, MB-Mecklenburg Bight, PB-Pomeranian Bight, and BS-Bornholm Sea. In the central Arkona Sea the stations AS1, AS2, and AS3, in the Bornholm Sea the station BS and and the Pomeranian Bight the station PB are indicated for later reference. The station AS1 corresponds to the monitoring station 113. The model area is indicated by the box.

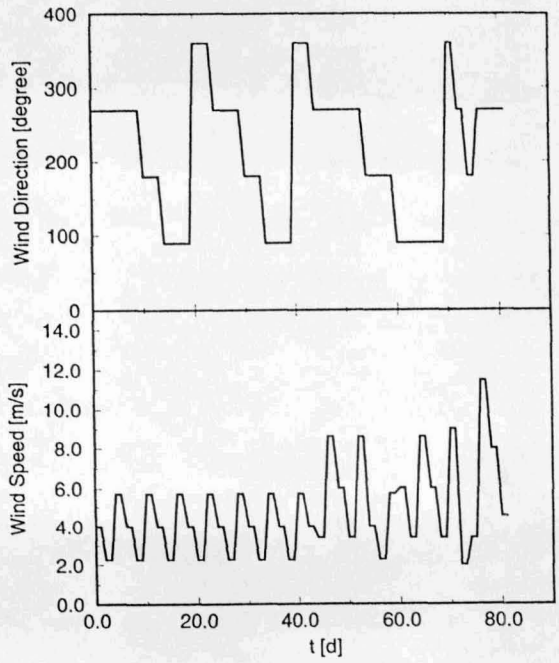

fig. 2: Time series of the synthetical wind used to the circulation model.

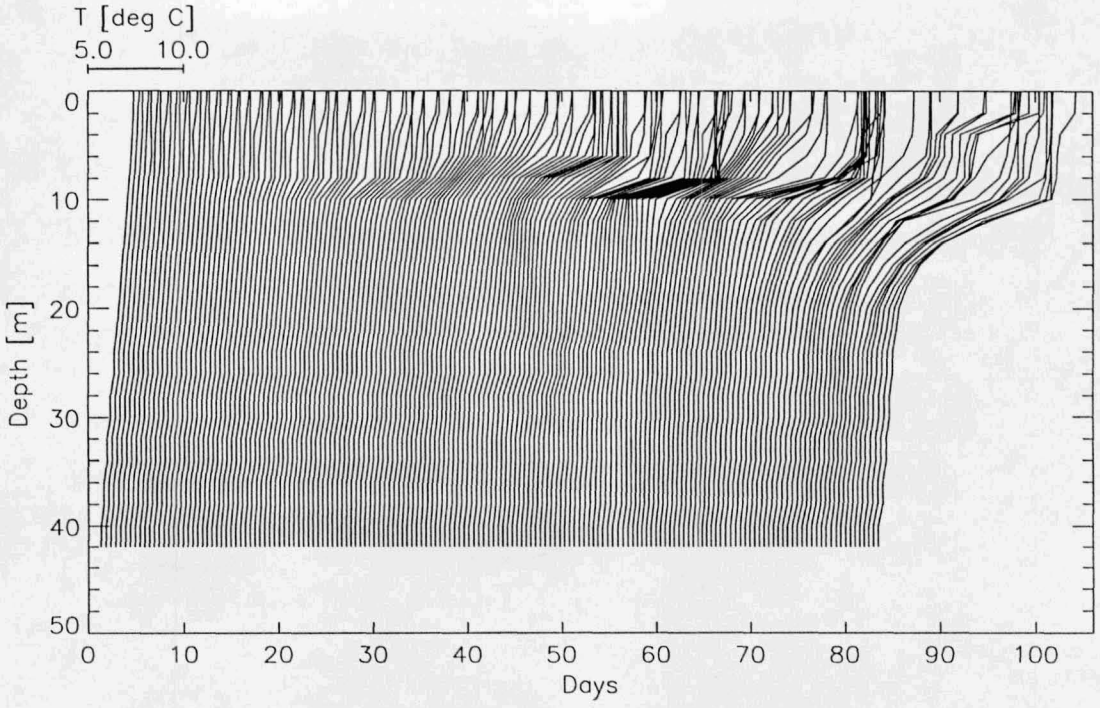

fig. 3: Time series of vertical model temperature profiles in the central Arkona Sea, at the station AS1.

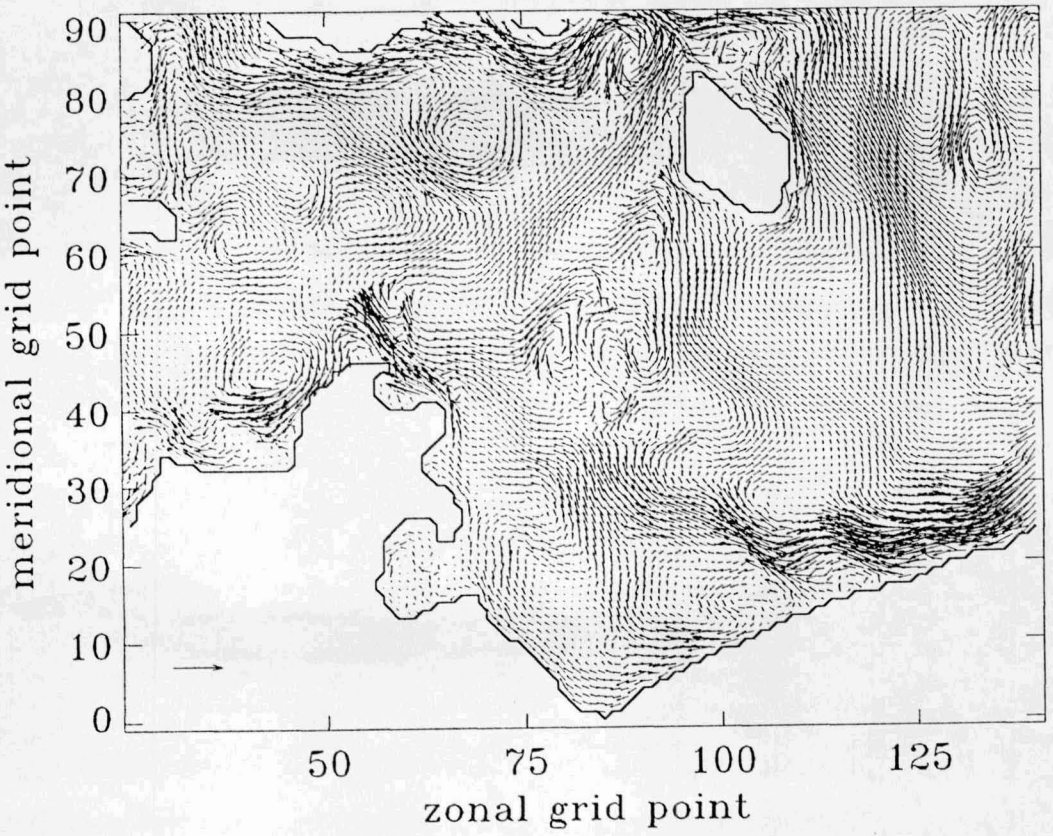
meridional grid point
0
10
20
30
40
50
60
70
80
90
50
75
100
125
zonal grid point

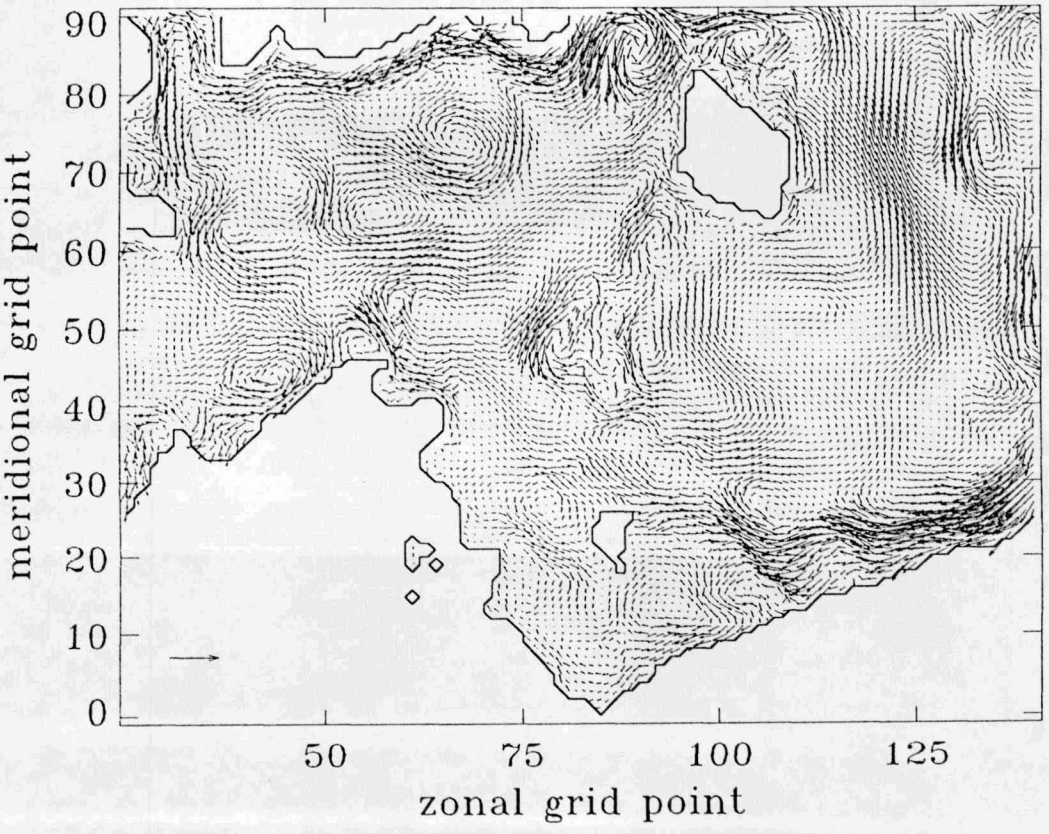
meridional grid point
0
10
20
30
40
50
60
70
80
90
50
75
100
125
zonal grid point

fig. 5: A series of snapshots of the surface distribution of model phytoplankton for (a) day 35, (b) day 38, (c) day 50, and (d) day 60.

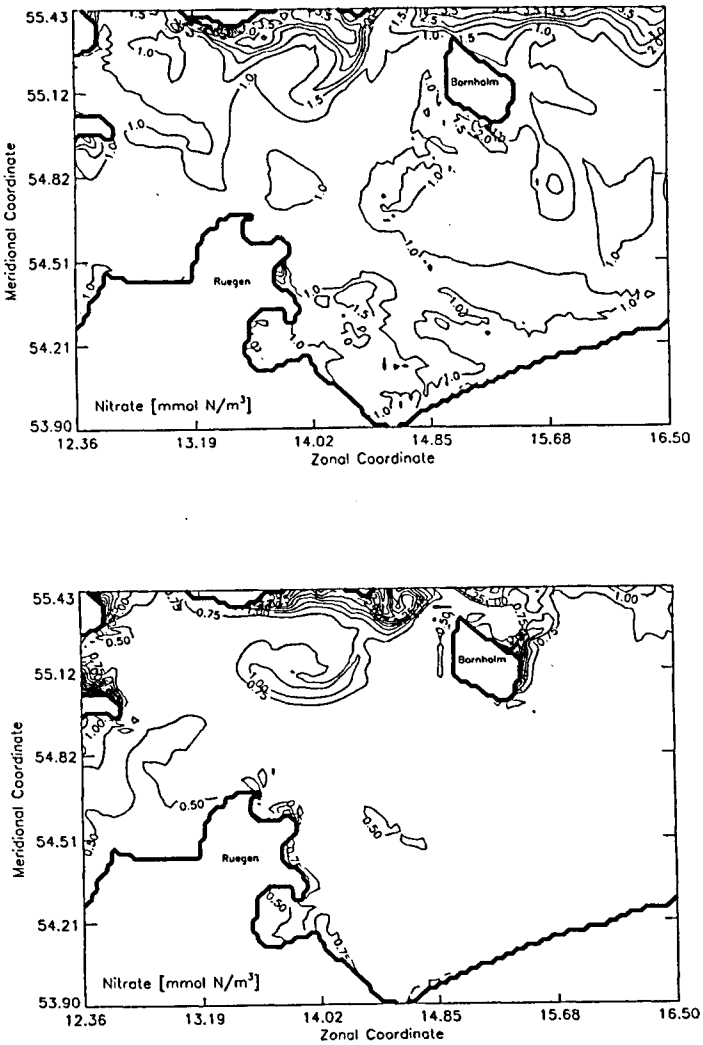

fig. 6: Nutrient distribution at the sea surface for day 51 (top) and day 60 (bottom).

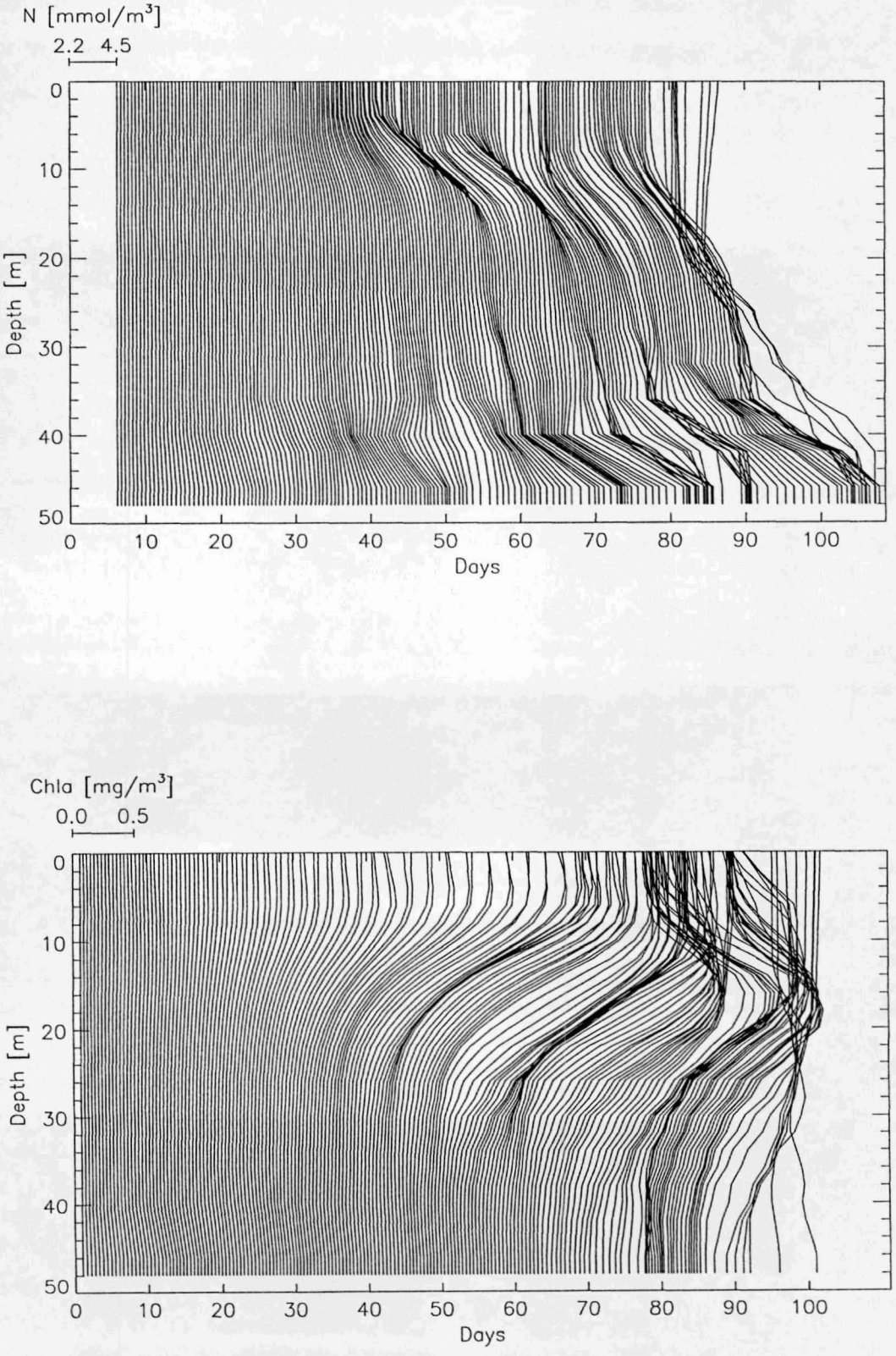

fig. 7: Time series of vertical profiles of the model nutrients (a) and phytoplankton (b) at the station AS1 in the Arkona Sea. The profiles are taken every 12 hours (midnight and noon) and subsequently shifted by a constant offset.

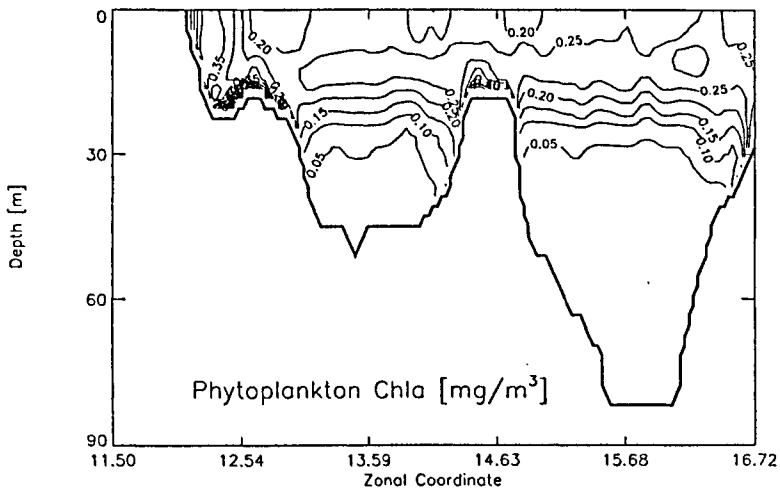

fig. 8: Zonal-vertical section of the plankton distribution along 54, 8°N at day 59 showing the deep plankton maximum in the thermocline. Note also the higher levels of P over the topographic features.

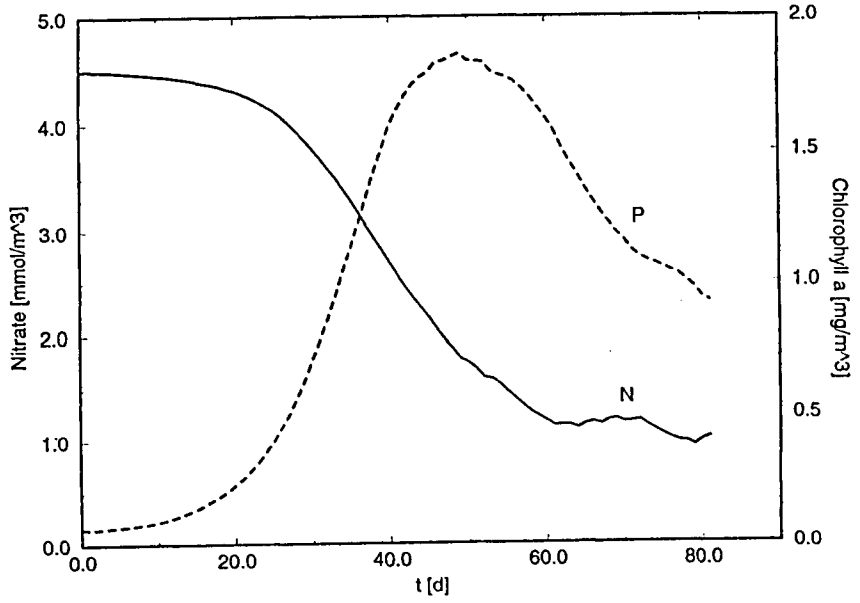

fig. 9: The temporal development of the concentrations of the model nutrients, N (solid), and model phytoplankton, P (dashed), integrated over the upper $14\,m$ of the whole model area.

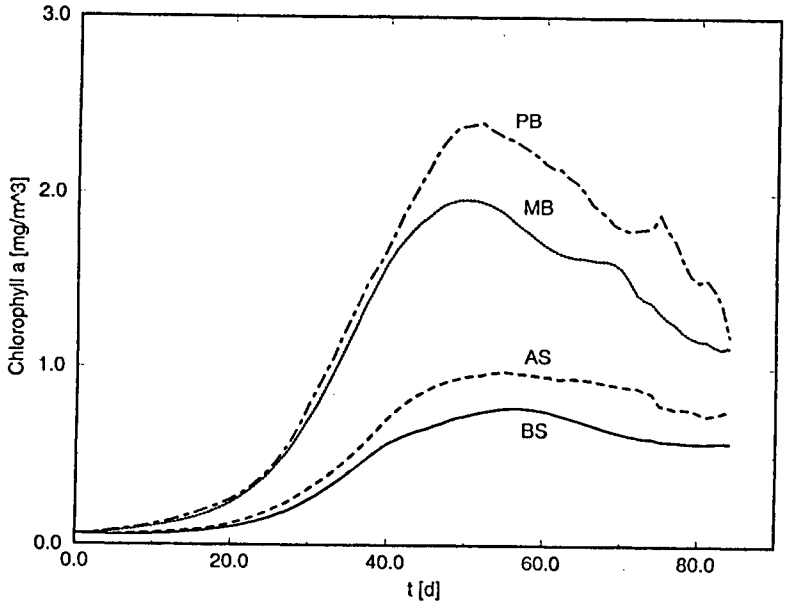

fig. 10: Development of the mean concentration of the model phytoplankton of the different sub-basins, Bornholm Sea (solid), Arkona Sea (dashed), Mecklenburg Bight (dotted), and Pomeranian Bight (dashed-dotted).

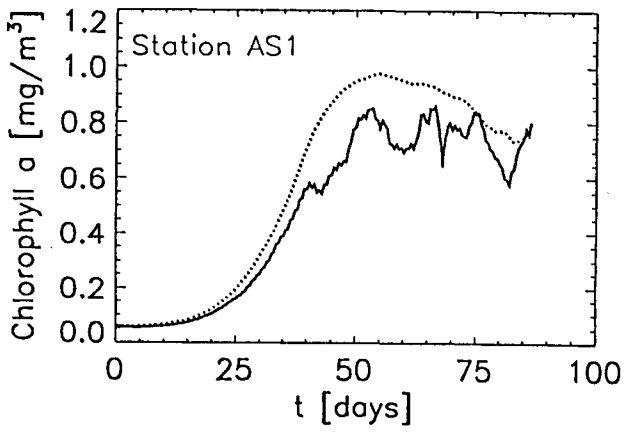

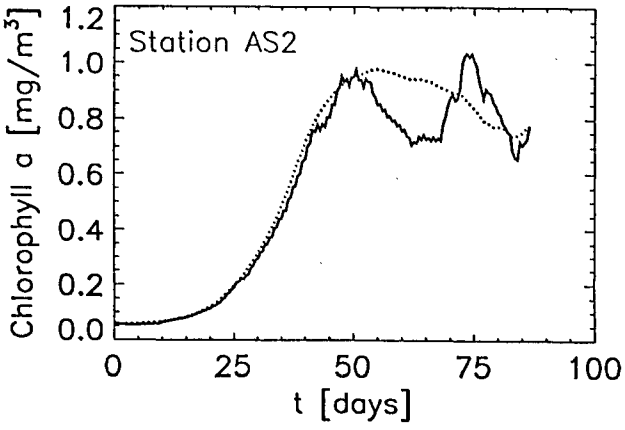

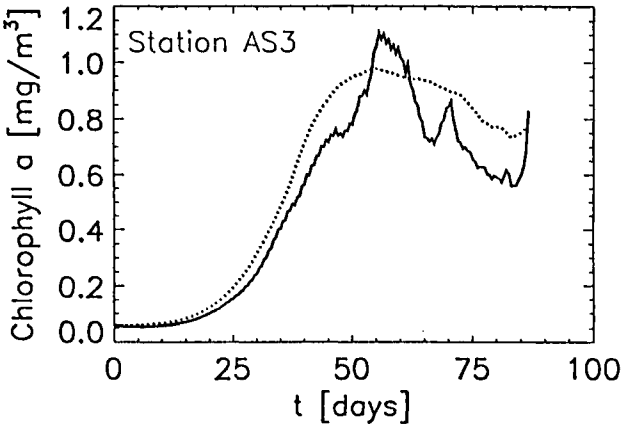

fig. 11: Time series of the mean value of the model phytoplankton in the Arkona Sea (dashed) and of the vertical means at the stations AS1, AS2, and AS3.

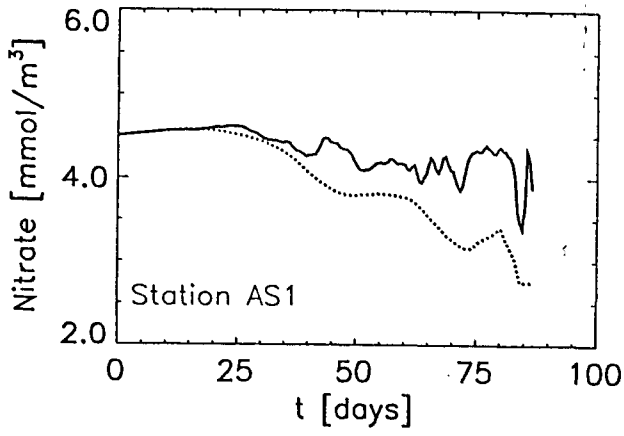

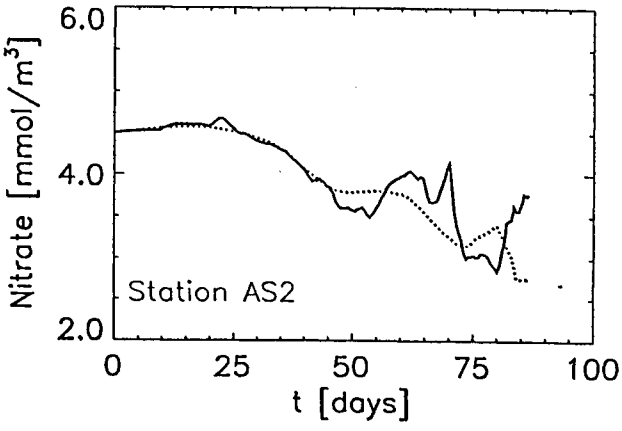

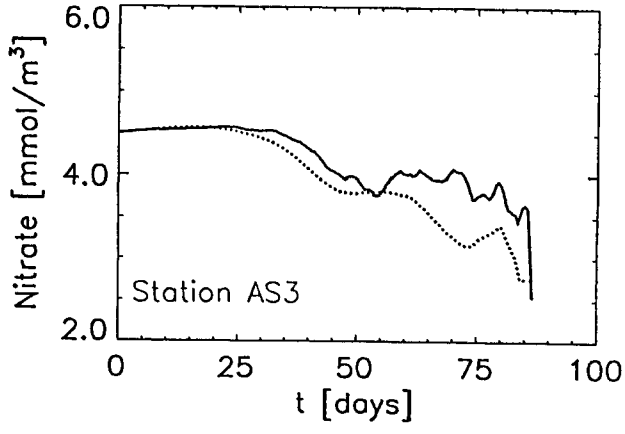

fig. 12: Time series of the mean value of the model nutrient concentration in the Arkona Sea (dashed) and of the vertical means at the stations AS1, AS2, and AS3.

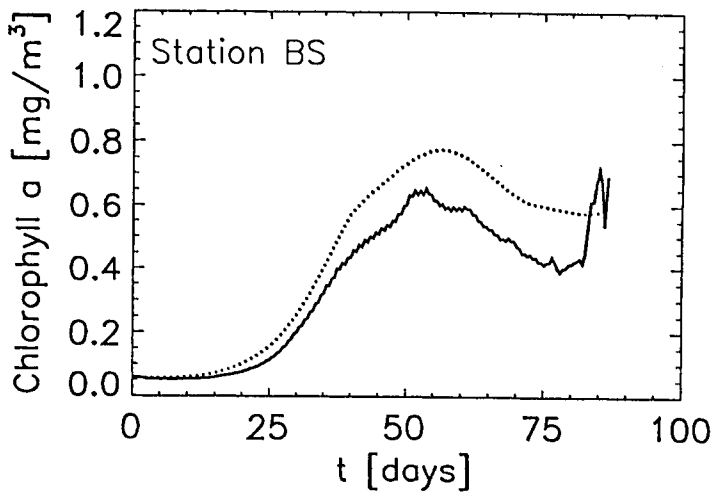

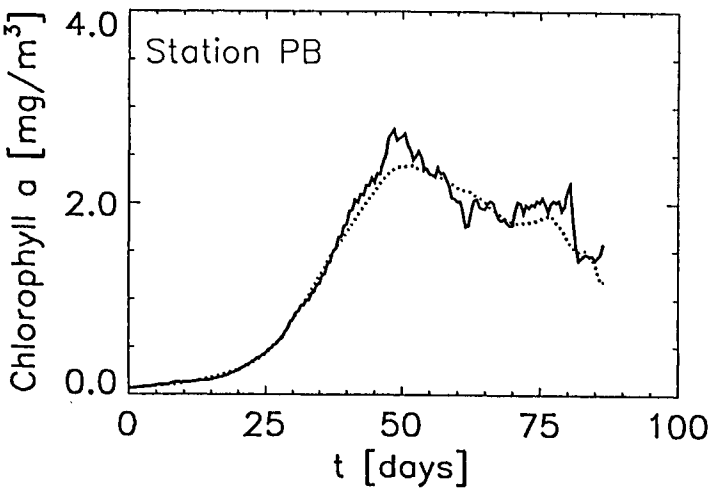

fig. 13: As fig. 11, but for the stations BS and PB.

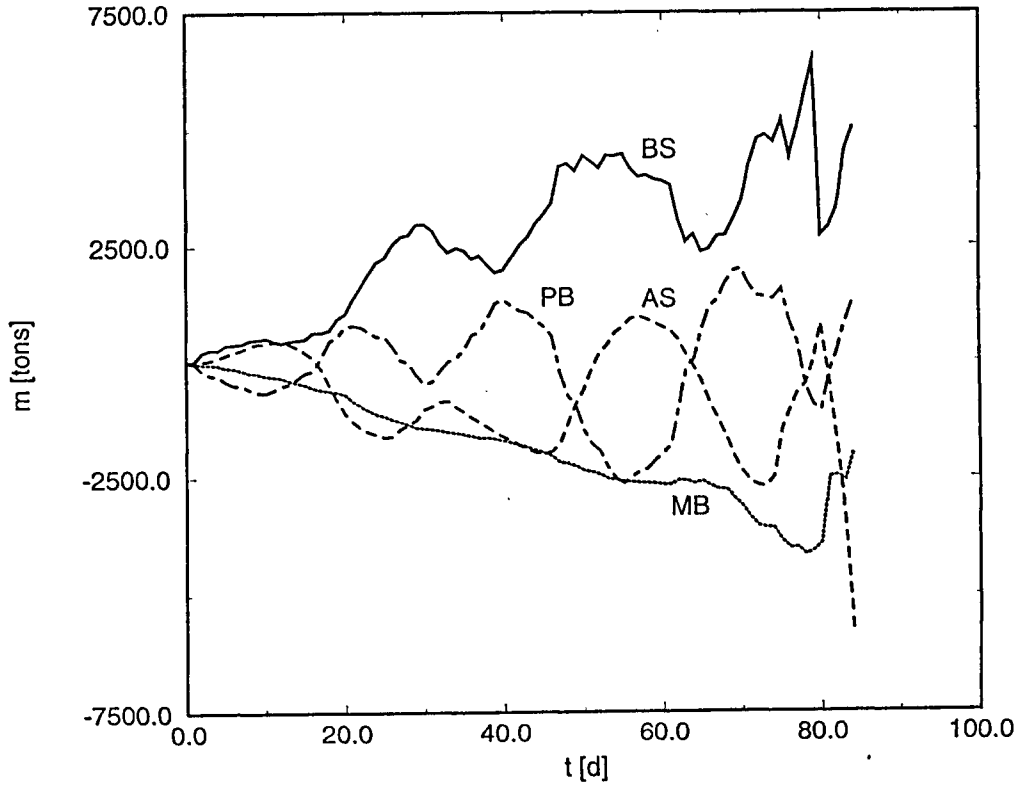

fig. 14: Temporal development of the differences of the total masses (in nitrogen) in the different sub-basins relative to the initial mass (BS-solid; AS-dashed, PB-point-dashed, MB-points).